Novel insights in growth of intermetallic compounds between Sn–3.0Ag–0.5Cu solder and flexible PCB substrates under strain

Xudong Zhang[1] · Xiaowu Hu[1] · Xiongxin Jiang[1] · Qinglin Li[2] · Liuru Zhou[1]

Abstract

The study investigated the effect of tensile and compressive strain on the interfacial reaction of SAC305/Cu system. Experimental results indicated that the thickness of Cu_6Sn_5 layer on non-strained samples slightly decreased after aging for 120 h and increased with prolonged aging time. The applied tensile strain had an enhanced effect on the growth of Cu_6Sn_5 phase, while the applied compressive strain inhibited the growth of Cu_6Sn_5 phase. However, the thickness of Cu_3Sn layer at SAC305/Cu solder joints increased gradually with increasing aging time, regardless of whether strain was or not applied on the solder joints. Besides, the mean diameter of Cu_6Sn_5 grain increased in three systems as the aging time was prolonged to 480 h. The morphology of Cu_6Sn_5 grain on non-strained samples gradually changed from round-shape into polyhedron-shape with increased aging time. The morphology of Cu_6Sn_5 grain under tensile or compressive strain was polyhedron-shape. The Kirkendall voids appeared within Cu_3Sn layer in three systems after aging for 120 h and the amount of voids increased gradually with prolonged aging time. The applied tensile or compressive strain had an enhanced effect on the formation of voids within Cu_3Sn layer and the enhanced effect of applied tensile strain was much remarkable than that of other systems.

1 Introduction

Flexible microelectronics has attracted much attention during the past years because of many advantages such as flexibility, light weight, small package volume, and so forth [1]. Flexible printed circuit board (FPCB), which is generally composed of a plastic substrate (polyimide etc.) coated with a conductive trace metal (Cu), is an important component in microelectronic packaging industry. Flexible PCB is generally bonded with Si chip by interconnecting solders with the usage of common reflowing technology and the solders as joining materials are widely used in microelectronics and electrical field. During reflowing, the solder melts and wets the Si chip and PCB sides. Simultaneously, an interfacial

reaction accompanying the formation of intermetallic compounds (IMCs) usually occurs at the solder/substrate interface [2, 3]. The thickness of IMCs layer gradually increases with increasing aging time and improving aging temperature [4]. It is well known that the thick IMCs layer could tend to initiate micro-cracks, leading to the reduction of mechanical properties [5], even the failure of solder joints. Therefore, it is essential to understand the interfacial reactions and the growth of IMCs of solder joint.

The eutectic Sn–Pb alloy was effectively replaced by eutectic Sn–Ag–Cu (SAC) alloy in soldering process due to the harm to environment and health resulted from heavy metal Pb and Pb-containing solders. In all of the SAC solders, the Sn–3.0 wt%Ag–0.5 wt%Cu (SAC305) solder had some favourable advantages of good wettability, mechanical properties and low melting point, which was considered as the most outstanding candidate to replace conventional Pb-containing solders [6–8]. A number of studies had been performed on SAC305 solder [9, 10]. Burke and Punch [9] had investigated the creep behaviour of join-scale SAC105 and SAC305 solder samples under shear conditions. SAC305 solder was superior for applications which featured thermo-mechanical fatigue because it accumulated less strain than SAC105 solder. Cheng et al. [10] discussed

✉ Xiaowu Hu
huxiaowu@ncu.edu.cn

1 Key Lab for Robot & Welding Automation of Jiangxi Province, Mechanical & Electrical Engineering School, Nanchang University, Nanchang 330031, People's Republic of China

2 State Key Laboratory of Advanced Processing and Recycling of Nonferrous Metals, Lanzhou University of Technology, Lanzhou 730050, People's Republic of China

the tensile properties of low Ag lead-free solder alloys. As reported that SAC305 solder possessed higher strength and lower elongation ration than SAC0307 and SAC105 solder alloys. Besides, many researchers had studied the interfacial reaction and shear strength of SAC305/Cu solder joint. The study of Hu et al. [11] indicated that the shear strength of SAC305/Cu solder joints increased with increased strain rate, while the thickness of IMC layer decreased. Bashir and Haseeb [12] discussed the effects of Ni nanopatricles doped flux on the mechanical properties and electrical resistance of SAC305 solder joints subjected to electromigration. As reported that the mechanical properties and electrical performance of SAC305/Cu improved after the addition of Ni nanopatricles.

Flexible PCB was usually used to reduce the packaging volume, which made the solder joints serve in strain state. Lin et al. [13] studied the interfacial reaction of Sn/Ag/Cu tri-layer on a deformed polyimide substrate. As found that applied strain (0.34%) resulted in different growth morphologies of Cu_6Sn_5 IMC. The blocky Cu_6Sn_5 formed at the Sn/Ag_3Sn interface subjected to compressive strain but rarely appeared at that subjected to tensile strain. Additionally, Lin et al. [14] also investigated the effect of larger strain (2.5%) on the Sn/Ag/Cu interface. They found that the growth rate of the Cu_6Sn_5 phase formed on the flexible PCB subjected to applied strain was enhanced regardless of the strain type, while the enhanced effect from compressive strain was more significant. Besides, Liao et al. [15] investigated the strain effect on the Sn/Ni interfacial reaction. They designed a three-point bending apparatus to bend the Sn/Ni bi-layer on a Si chip. The results revealed that both tensile and compressive strains (0.069%) improved the growth rate of the Ni_3Sn_4 phase. Chen and Chen [16] found that the tensile stress could significantly mitigate the growth of Sn whisker and hillock on the Sn thin film.

Even though numerous research had been made to study the interfacial reactions of solder joints under compressive or tensile strain, less attention has been paid to on the influence of different strain values to SAC305/Cu solder joints. Therefore, the study focused on the interfacial reaction and IMC growth between SAC305 solder and FPCB pad with a 35 μm Cu layer under various compressive or tensile strain values.

2 Experimental produces

A commercial FPCB (Shenzhen V-Layers, China), a 25 μm thick polyimide (PI) pad coated with a 35 μm thick Cu layer, was used as the substrate. The SAC305 solder foil with 90 μm in thickness was placed on the Cu layer using rosin mildly activated flux. Figure 1 shows the schematic drawing of SAC305/Cu/PI system subjected to applied strains. The SAC305/Cu solder joints on PI were prepared through the reflowing process in a reflow oven, in which the specimens were reflowed at 250 °C for 10 min. The strained experiments were performed by sticking the specimens tightly on the ceramic rod, as shown in Fig. 1. If SAC305 solder side was stuck tightly on the ceramic rod, the SAC305/Cu solder joint between PI board and the neutral plane was subjected to tensile strain, as shown in Fig. 1(A). On the contrary, if the PI board side was stuck tightly on the ceramic rod, the SAC305/Cu solder joint between PI board and the neutral plane was subjected to compressive strain, as shown in Fig. 1(B). The diameter of ceramic rod was 5 mm, 10 mm, 15 mm and 20 mm. According to literature [15], the applied strain value was calculated by the thickness of experiment samples and the radius of curvature. In the experiment, the radius of curvature was the radius of the ceramic rod. The applied strain value could be obtained using Eq. (1):

Fig. 1 Schematic drawing of the SAC305/Cu/PI subjected to applied strains (Color figure online)
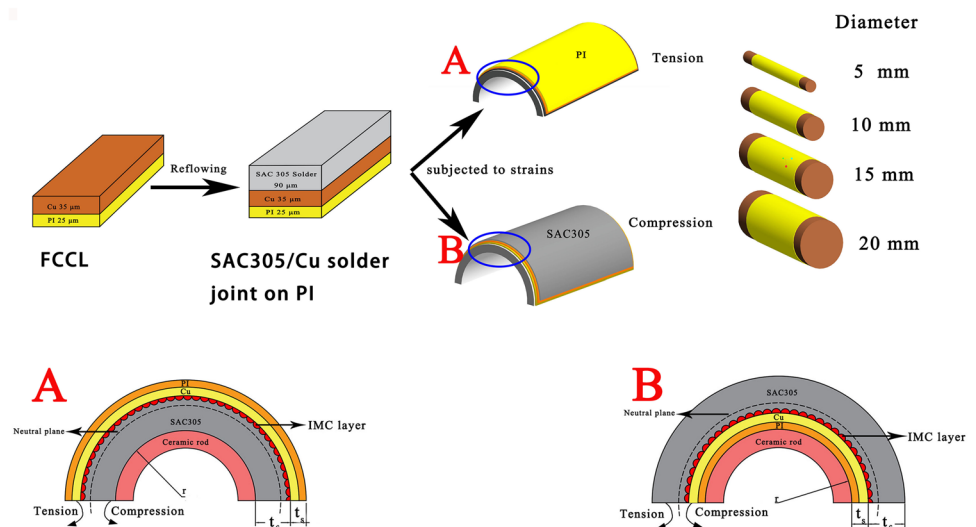
$$\varepsilon = \frac{t_s + t_f}{2r} \tag{1}$$

where r was the radius of ceramic rod, t_s and t_f was the thickness of the FPCB pad and SAC305 solder foil, respectively. Taking the known parameters ($t_s = 60$ μm and $t_f = 90$ μm) into Eq. (1). The strain near the neutral plane was regarded as the applied strain of SAC305/Cu solder joints, hence the applied strain was calculated to be 1.5%, 0.75%, 0.5% and 0.375%, respectively. The solid-state aging was conducted by placing the strained FPCB stuck on the ceramic rod in an oven at 150 °C for 24–480 h. Another set of FPCBs without any applied strain was aged as a reference.

After solid-state aging, the partial specimens were treated metallographically. This partial specimens were mounted in epoxy resin, following by grounding with SiC paper and polishing with the 2.5 μm and 0.5 μm diamond paste in the direction perpendicular to SAC305/Cu interface. In order to observe the top view of IMC, the other partial specimens were etched in a solution of 10% HNO_3 + 90% CH_3OH for 1 min to dissolve the remaining solder. The interfacial structures of samples and morphologies of interfacial IMC grains were observed by scanning electron microscopy (SEM). An X-ray microanalysis using energy dispersive spectroscopy (EDS) allowed the SEM to qualitatively analyze the elements present in a selected area of backscattered electron image. The average thickness of the IMCs was determined by dividing the cross-sectional area of the IMCs by the linear length of the interface [17].

3 Results and discussion

Figure 2 shows the interfacial cross-section SEM micrographs of SAC305/Cu solder joints before aging. It could be seen that the scallop-type Cu_6Sn_5 layer existed at the SAC305/Cu interface. The Cu_3Sn layer did not be found at the SAC305/Cu interface. In addition, the thickness of Cu_6Sn_5 layer was 2.67 μm.

Figure 3 shows the interfacial cross-section SEM micrographs of SAC305/Cu solder joints after aging at 150 °C for 24–480 h. The samples in Fig. 3a1–a5 were not subjected to any strain. The samples in Fig. 3b1–c5 were subjected to tensile strain. The applied strain values in Fig. 3b1–b5 and c1–c5 were 0.375 and 0.5%, respectively. Figure 3d1–e5 was this samples subjected to compressive strain. The applied strain values in Fig. 3d1–d5 and e1–e5 were 0.75 and 1.5%, respectively. According to the element analysis results in Fig. 4, the phase adjacent to the Cu side was identified to be Cu_3Sn, the phase next to the SAC305 solder side was Cu_6Sn_5, the embedded phase in the Cu_6Sn_5 layer was Ag_3Sn. This indicated that the applied strain, regardless of whether the strain state was compressive or tensile, did not alter
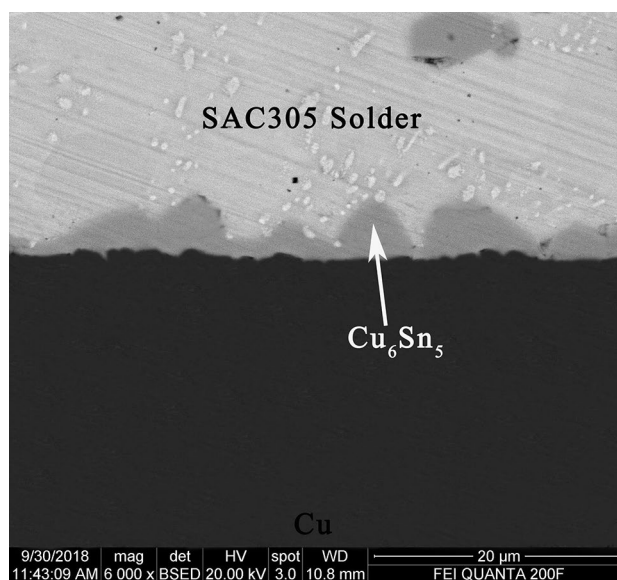
Fig. 2 Cross-sectional SEM micrographs of SAC305/Cu interface on FPCB after reflowing at 250 °C for 10 min

the type of IMCs formed at the SAC305/Cu interface. It was consistent with the study of Li et al. [18], in which the Cu_6Sn_5, Cu_3Sn and Ag_3Sn IMC formed at the SAC305/Cu interface after aging for 250 h and the elemental mapping analysis of SAC305/Cu interface without strain aged at 150 °C for 480 h was made to know the distribution of each element, as shown in Fig. 5. It was clearly seen that the Sn and Ag atoms were mainly concentrated in the solder matrix, while the Cu atoms mainly were aggregated in the upper layer of FPCB. With the interdiffusion of atoms, the reaction of three atoms resulted in the formation of three types of chemical substance, which were identified as Cu_6Sn_5, Cu_3Sn and Ag_3Sn.

Figure 3a1 shows the interface of SAC305/Cu solder joint without strain aging for 24 h. It was clearly found that the scallop-type IMC layer, which was identified as the the Cu_6Sn_5 phase by EDS, existed at the SAC305/Cu interface. However, a new IMC layer was observed between Cu_6Sn_5 layer and Cu when the SAC305/Cu solder joint was subjected to tensile or compressive strain with the same aging time of 24 h. The EDS result revealed that the new IMC layer was Cu_3Sn layer. This illustrated the strain, both tensile and compressive, could promote the formation of Cu_3Sn phase. Further increasing the aging time to 120 h, there were two IMCs layer (Cu_6Sn_5 and Cu_3Sn) existed at the SAC305/Cu interface in three systems, as seen in Fig. 3a2–e2. It indicated that the Cu_3Sn phase also gradually formed at the SAC305/Cu interface of non-strained sample with the prolonged aging time. Tu [19] found that the Cu_6Sn_5 IMC formed firstly at the Sn-based solder/Cu interface, because Cu_6Sn_5 phase had lower activation energy compared to the
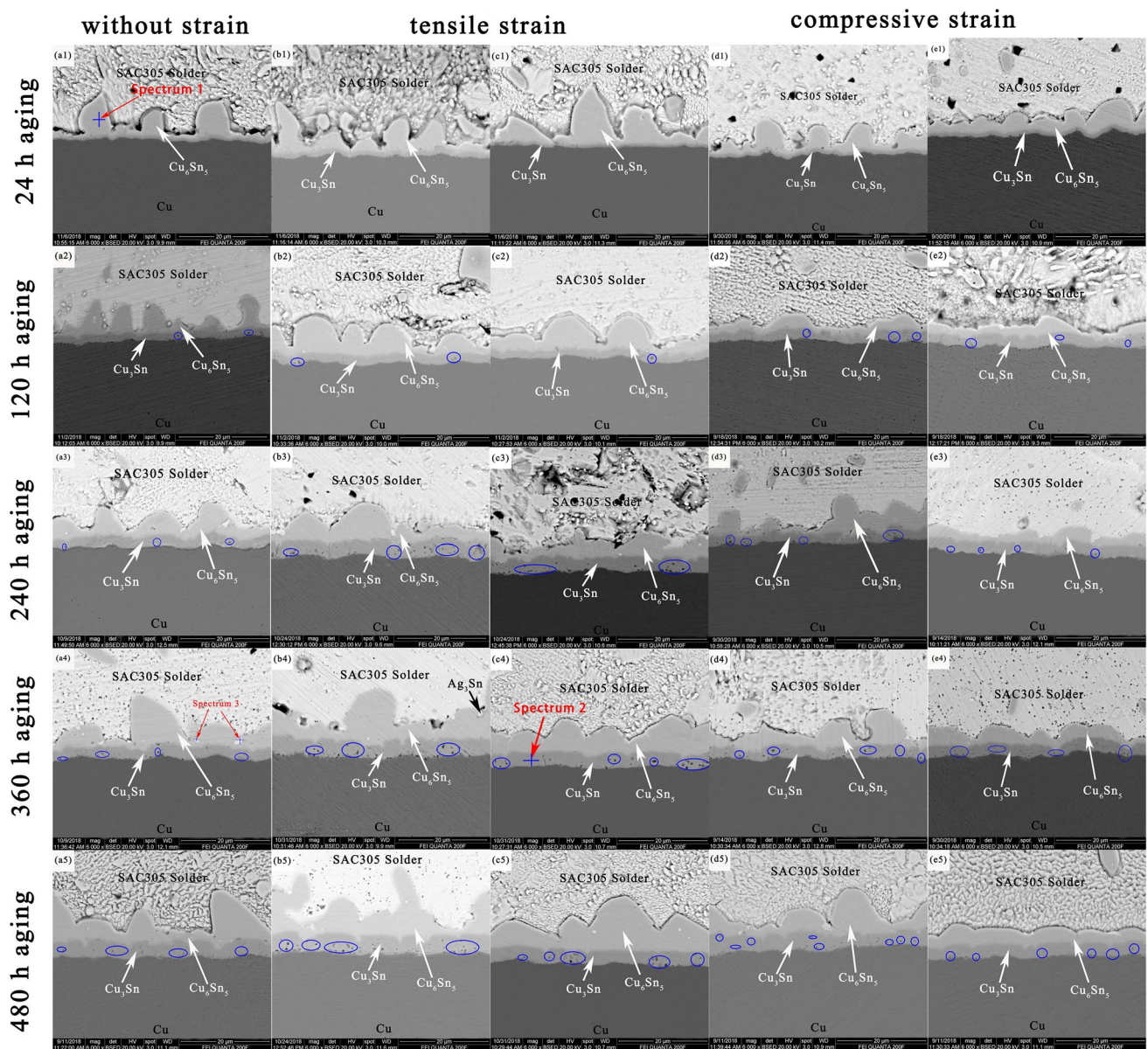
Fig. 3 Cross-sectional SEM micrographs of SAC305/Cu interface on FPCBs with different applied strains after isothermal aging at 150 °C for 24–480 h: **a1**–**a5** without strain, **b1**–**c5** tensile strain and **a3**–**e5** compressive strain

Cu_3Sn phase. Then the Cu_3Sn IMC layer would form over time by consuming the Cu_6Sn_5 IMC layer. This was because the Cu_6Sn_5 IMC layer was thermodynamically unstable.

Another worthy noticed phenomenon observed in Fig. 3 was the formation of voids at the SAC305/Cu interface after aging treatment, especially within the Cu_3Sn layer. After aging for 24 h, voids were not observed at the interface regardless of whether strain was or not applied. The voids gradually formed within the Cu_3Sn layer as the aging time was prolonged to 120 h. According to many studies [20–23], these voids are identified as the Kirkendall voids. The formation of voids are due to the difference of interdiffusion

coefficients between different atoms at the interface. Literature by Wang et al. [24] reported that the formation of voids needed two steps. Firstly, the unbalance inter-diffusion of Cu and Sn atoms resulted in lots of vacancies at the Cu_3Sn layer. Secondly, these vacancies would get together and coalesce into voids. As seen in Fig. 3, the amount of voids within Cu_3Sn layer increased gradually with increased aging time. Besides, it could be clearly seen that the applied tensile strain had an enhanced effect on the formation of voids and the phenomenon was more obvious with increased aging time. This could be attributed to the thicker total IMC layer under tensile strain condition. It was well known that the Sn

Fig. 4 EDS analysis of IMC layer in Fig. 3, **a** spectrum 1 in Fig. 3a1, **b** spectrum 2 in Fig. 3c4, **c** spectrum 3 in Fig. 3a4
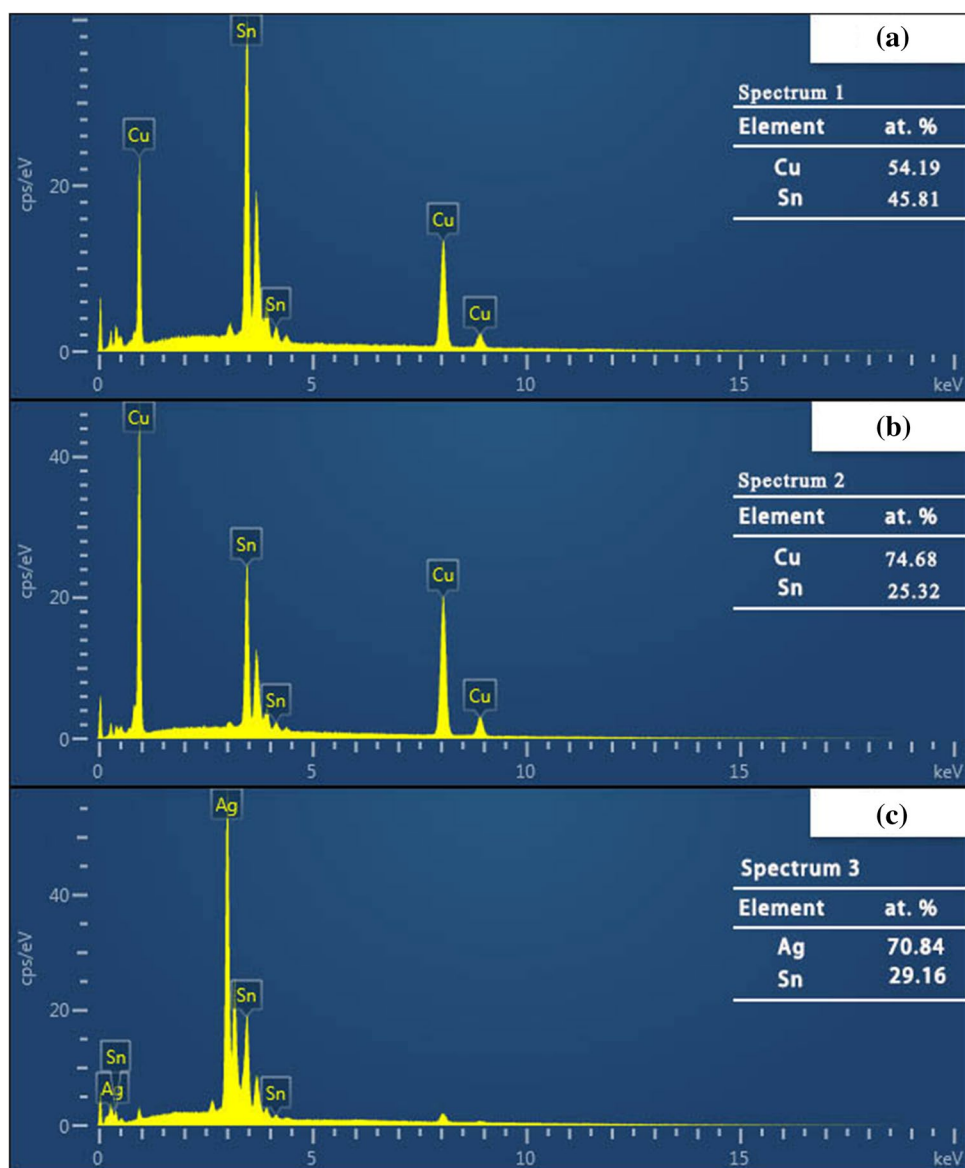
atom in the SAC305 solder was consumed to diffuse across the IMC layer to react with Cu atom. The thicker IMC layer had more significant effect of inhibition on the diffusion of Sn atom, resulting in larger difference of interdiffusion coefficients between Sn and Cu atoms. Additionally, the amount of voids within Cu_3Sn layer obviously increased when the SAC305/Cu solder joints were subjected to compressive strain. The reason of difference is explained by the fact that the applied compressive strain enhances the difference of interdiffusion coefficients between Sn and Cu atoms. Generally, during reflowing and aging process, the Sn atom diffused to the Cu side and reacted with the Cu atom to form the Cu_6Sn_5 IMC. Song et al. [25] found that the formation of Cu_6Sn_5 IMC would produce volume change ($\Delta V = V_{Cu\,6\,Sn5} - 6V_{Cu\,(with\,5\,Sn)} = +75.41 cm^3/mol$), which resulted in volume expansion at the Sn/Cu interface.

The volume expansion would cause intrinsic compressive stress at the interface. In order to release the intrinsic compressive stress, the Cu atom diffused rapidly toward the Sn side. In other word, the formation of Cu_6Sn_5 IMC could improved the diffusion rate of Cu atom from Cu layer to SAC305 solder. In present study, the intrinsic compressive stress still occurred at the SAC305/Cu interface during reflowing and aging process, as seen in Fig. 6. As a result, the applied external compressive strain on the FPCB pad further enhanced the intrinsic compressive stress. As shown in Fig. 6, the stronger compressive stress could act as a driving force for out-diffusion of Cu atom towards the SAC305 solder basing on the Le Chatellier's theory [26]. Therefore, the difference of interdiffusion coefficients between Sn and Cu atoms was expanded by the compressive stress, resulting in the increasing of voids.

Figure 7 shows the total thickness of the IMCs formed on the FPCBs with and without applied strain as a function of aging time. It could be clearly seen that the total thickness of IMCs layer gradually increased with prolonged aging time in three systems. In Fig. 7a, the total IMCs layer on the tensile strained FPCBs was thicker than that of the non-strained FPCB, regardless of the strained value. It was consistent with the study of Lin et al. [14], in which the grow rate of
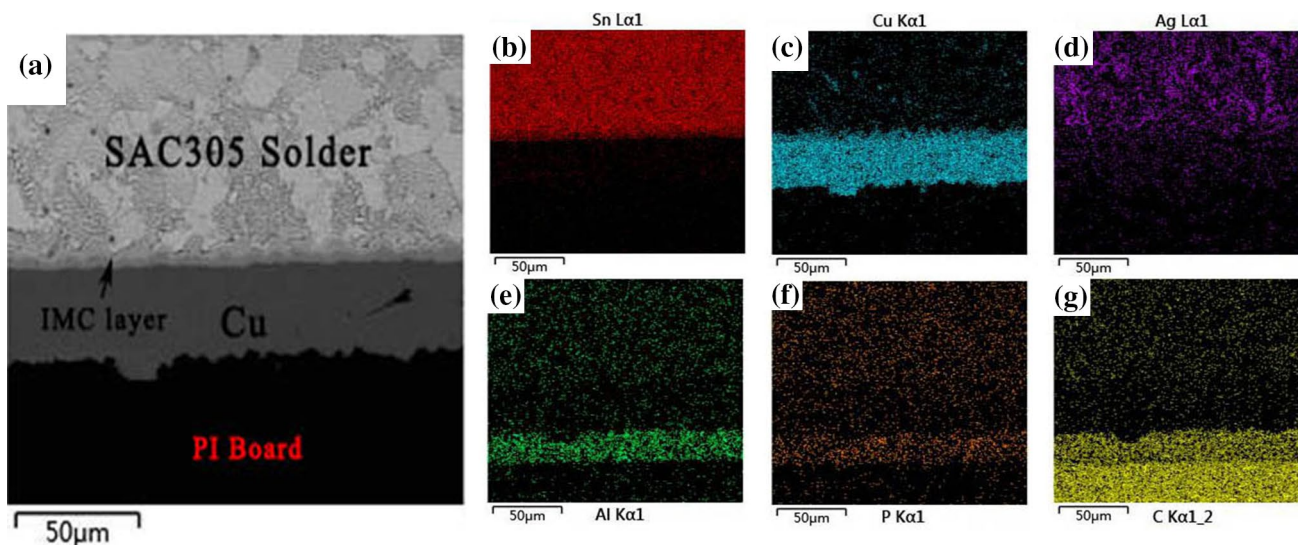

Fig. 5 The SEM image and elemental mapping analysis of the SAC305/Cu interface without strain aged at 150 °C for 480 h
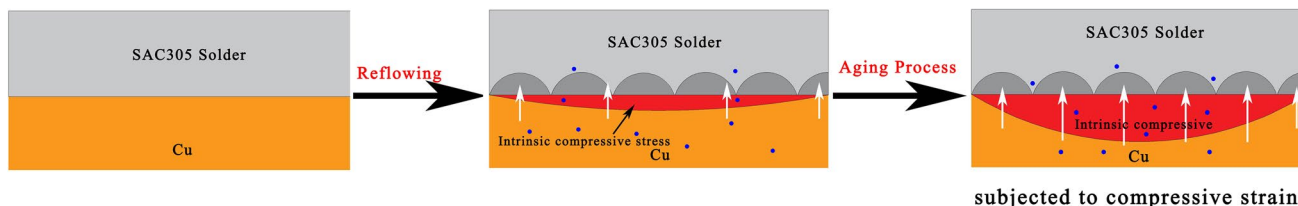

Fig. 6 Schematic drawing showing that the variation of internal compressive stress subjected to different strain type. White arrows indicate Cu dissolution through the interface; Red area indicate the range of intrinsic compressive stress; Blue circles indicate the Cu atoms (Color figure online)
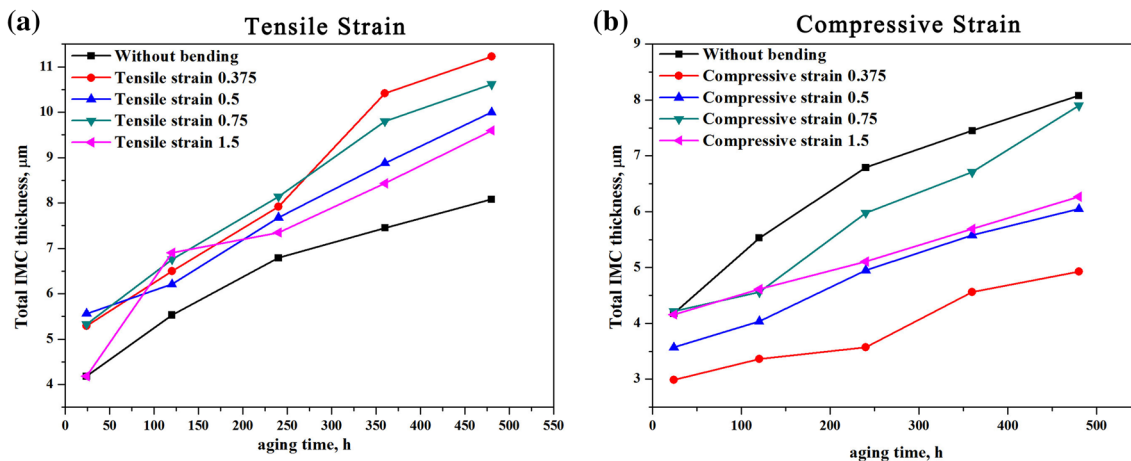

Fig. 7 Total thickness of IMCs formed at the SAC305/Cu interface on FPCBs with and without applied strain after aging at 150 °C for various lengths of time: **a** tensile strain and without strain, **b** compressive strain and without strain

IMC layer formed on the FPCB subjected to tensile strain was enhanced. It was obviously seen that the total interfacial IMCs layer of the FPCBs with tensile strain of 0.375% was thicker than that of other strained value when the aging time was up to 360 h. In Fig. 7b, the total IMCs layer on the compressive strained FPCBs was thinner than that of the non-strained FPCB. Meanwhile, when the compressive strain value was 0.375%, the total thickness of IMC layer on the tensile strained FPCB was the thinnest. Figure 8 shows the growth trend of the total IMC layer at the SAC305/Cu interface as the strain value increased from 0 to 1.5%. As seen in Fig. 8a, the total IMC layer of non-strained samples within the same aging time was thinner than that of other tensile strained samples. In Fig. 8b, it could be clearly found that the 0.375% compressive strained system had the thinnest IMC layer in all compressive strained systems. According to the Nabarro–Herring model [27], the vacancy concentration in a region subjected to compressive reduces to below the equilibrium vacancy concentration. Therefore, the model indicated that the applied compressive strain resulted in lower vacancy concentration in the interfacial reaction region, which weakened the atomic diffusion of Sn and Cu atoms. In contrast, the applied tensile strain resulted in higher vacancy concentration, enhancing the atom diffusion. Hence, the growth rate of IMCs layer under tensile strained condition was enhanced due to the existence of more vacancies. The fewer vacancies within total IMC layer on the compressive strained samples led to the reduction of growth rate of IMCs layer.

Figure 9 shows the thickness of individual Cu_6Sn_5 and Cu_3Sn IMC layer, respectively, as a function of aging time. The thickness of individual Cu_6Sn_5 IMC layer under tensile or compressive strain were shown in Fig. 9a, c, respectively. It could be clearly seen that the applied tensile strain had an enhanced effect on the growth rate of Cu_6Sn_5 phase,

while the applied compressive strain inhibited the growth of Cu_6Sn_5 phase. The thickness of Cu_6Sn_5 IMC layer on FPCB pad without strain decreased slightly after aging for 120 h and increased constantly with prolonging aging time to 480 h. When the FPCBs pad were subjected to tensile strain, the thickness of Cu_6Sn_5 IMC layer presented different variation trend with different strain value. The variation trend of Cu_6Sn_5 IMC layer thickness was the same as that of non-strained FPCB when the tensile strain value was 0.5 or 0.75%. However, when the strain value increased to 0.375 or 1.5%, the thickness of Cu_6Sn_5 IMC layer increased after aging for 120 h and decreased slightly with prolonging aging time to 240 h. The variation trend of Cu_6Sn_5 IMC layer thickness on FPCBs subjected to 0.75 or 1.5% compressive strain was similar to that of non-strained FPCB. It is worthy noticed that the thickness of Cu_6Sn_5 IMC layer under 0.375% compressive strain was not almost increased. The thickness of individual Cu_3Sn IMC layer under tensile or compressive strain were shown in Fig. 9b, d, respectively. It could be clearly seen that the Cu_3Sn IMC layer increased gradually with the increased aging time, regardless of the strain was or not applied on FPCB. Hence, the growth of Cu_3Sn phases made a significant contribution to the increased thickness of the total IMC layer. In particular, the increased thickness of the total IMC layer was primarily provided by the growth of Cu_3Sn phase when the compressive strain value was 0.375%.

As it is well known that the formation and growth of Cu_3Sn phase were resulted from following reaction [28]:

$$Cu_6Sn_5 + 9Cu \rightarrow 5Cu_3Sn \tag{2}$$

It could be deduced that the reduction of Cu_6Sn_5 IMC layer thickness during aging time might be attributed to the rapidly increased thickness of Cu_3Sn IMC layer. In other word, the growth rate of Cu_3Sn phase during this aging time was faster than that of Cu_6Sn_5 phase. Therefore, the
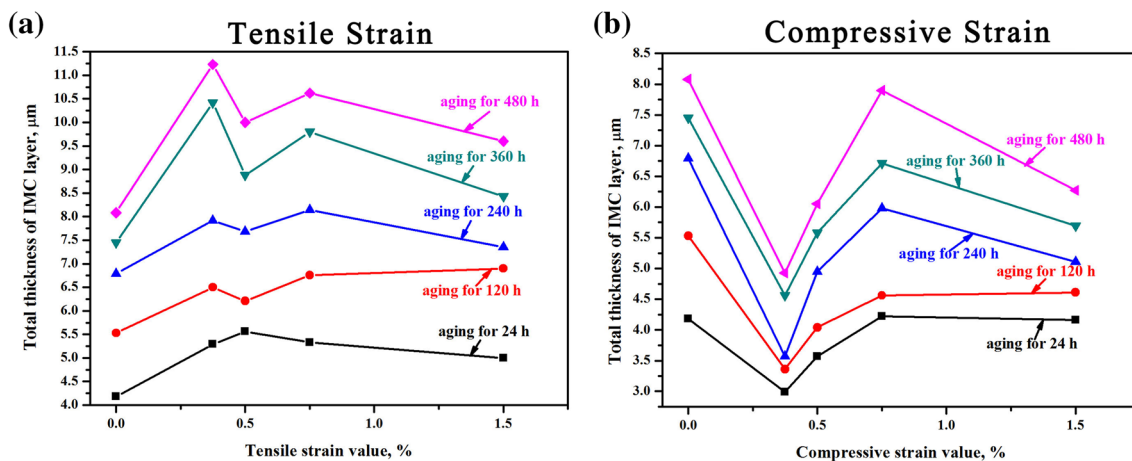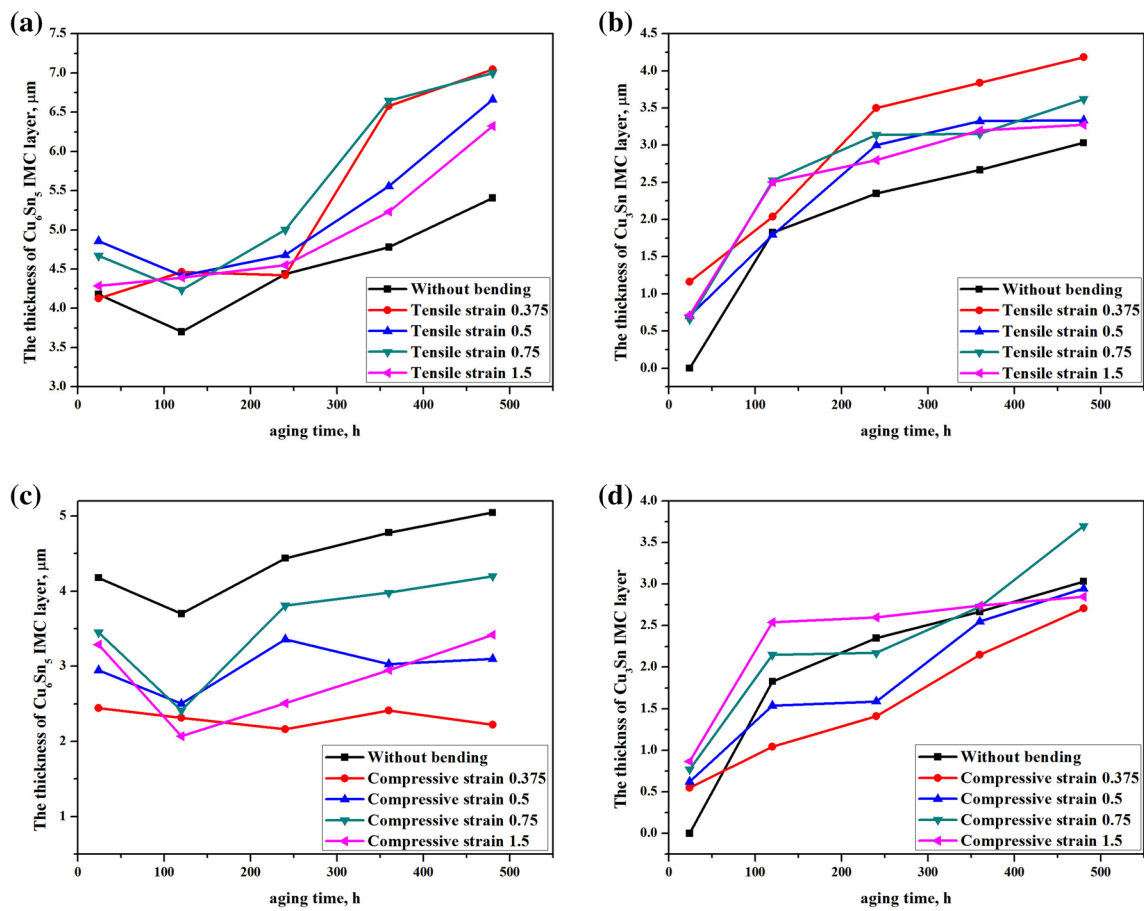

Fig. 8 Relationships of total thickness of IMC layer at the SAC305/Cu interface with strain value: **a** tensile strain, **b** compressive strain

Fig. 9 The thickness of Cu_6Sn_5 and Cu_3Sn IMC layer at the SAC305/Cu solder joints on FPCBs with and without applied strain after aging at 150 °C for various lengths of time: **a**, **b** tensile strain and without strain, **c**, **d** compressive strain and without strain

Table 1 The mean diameter of Cu_6Sn_5 IMC grains at the SAC305/Cu solder joints subjected to tensile strain at 150 °C for different aging time

Strain value	The mean diameter of Cu_6Sn_5 IMC grains/μm				
	24 h	120 h	240 h	360 h	480 h
0	3.32	5.77	7.68	9.19	10.52
0.375	7.11	8.02	8.71	9.51	10.29
0.5	7.06	7.52	8.08	9.24	10.09
0.75	7.65	8.11	8.86	9.65	10.49
1.5	8.29	8.64	9.04	10	10.69

Table 2 The mean diameter of Cu_6Sn_5 IMC grains at the SAC305/Cu solder joints subjected to compressive strain at 150 °C for different aging time

Strain value	The mean diameter of Cu_6Sn5 IMC grains/μm				
	24 h	120 h	240 h	360 h	480 h
0	3.32	5.77	7.68	9.19	10.52
0.375	6.25	6.47	7.52	7.73	8.91
0.5	6.45	7.13	7.67	8.16	9.04
0.75	6.98	7.36	8.38	8.82	9.53
1.5	6.57	7.72	7.82	8.74	10.11

formation of Cu_3Sn phase after aging for 24 h was attributed to the effect of compressive or tensile strain, improving the rate of Cu atom diffusion towards the Cu_3Sn phase.

It is well known that the aging time plays an important role in the growth of Cu_6Sn_5 IMC grain. According to previous studies [17, 29–31], the Cu_6Sn_5 IMC grain gradually became large with increased aging time. Tables 1 and 2 show the mean diameter of Cu_6Sn_5 IMC grains on FPCBs

subjected to tensile and compressive strain, respectively. It could be seen that the mean diameter of Cu_6Sn_5 IMC grains at the SAC305/Cu solder joints without strain increased obviously as the aging time was increased to 480 h, which was in agreement with the result of corresponding cross-sectional images (as shown in Fig. 3a1–a5). Besides, when the SAC305/Cu solder joints on FPCBs subjected to tensile stress were aged for 24 h, the mean diameter of Cu_6Sn_5

IMC grains obviously increased. The result was consistent with the thickness of Cu_6Sn_5 IMC layer (Fig. 9a). According to Table 1, the Cu_6Sn_5 IMC grains on tensile strained FPCB pad gradually grew as the aging time was increased to 480 h, but the grow rate was remarkably slower than that of non-strained FPCB pad. Interestingly, the mean diameter of Cu_6Sn_5 IMC grains obviously increased when the 24 h-aged SAC305/Cu solder joints on FPCBs were subjected to compressive strain, but the corresponding thickness of Cu_6Sn_5 IMC layer was thinner than that of non-strained FPCB (Fig. 9c). Due to the specificity of Cu_6Sn_5 IMC layer thickness on the 0.375% strained FPCBs, the morphology of Cu_6Sn_5 grains was shown in Fig. 10. The morphology of interfacial Cu_6Sn_5 grains at the SAC305/Cu solder joints without strain were round-shape after aging for 24 h (Fig. 10b1). For the aged solder joints, the morphology of Cu_6Sn_5 gradually changed from round-shape into polyhedron-shape. However, the morphology of Cu_6Sn_5 grains on the 0.375% tensile stained FPCB (Fig. 10a1) were polyhedron-shape after aging for 24 h. The morphology of Cu_6Sn_5 grains did not obviously change and the grains size increased slightly with prolonged aging time. It worthy noticed that the morphology of Cu_6Sn_5 grains on the 0.375% compressive strained FPCB was slightly loose, as seen in Fig. 10c1 and c2. This might lead to the thinner Cu_6Sn_5 IMC layer, compared to that of non-strained FPCB. The growth of Cu_6Sn_5 grains is because of two kinetic processes, one is ripening and another is interfacial reactions [32]. The ripening process of Cu_6Sn_5 grains is the result of reaction between Cu_6Sn_5 grains, in which the grains grow larger in size and the number of Cu_6Sn_5 grains reduces over time. As shown in Fig. 10, the surfaces of the two adjacent grains were coherent and the diffusional interaction between grains became a larger grain. That resulted that some grains with adjacent side surfaces would merge together, as indicated as the marked blue circles in Fig. 10a2, b3 and c3. Additionally, there were some white micro-particles, which were identified to be Ag_3Sn phase formed in the solder bulk, existed on the surface of Cu_6Sn_5 grains.

4 Conclusions

The study has investigated the effect of different tensile or compressive strain values on the interfacial reaction of SAC305/Cu solder joints. Based on the experimental results

Fig. 10 The morphology of SAC305/Cu interfacial Cu_6Sn_5 phase formed on different strain state aged at 150 °C for 24, 240 and 480 h, **a1–a3** tensile strain 0.375; **b1–b3** without strain and **c1–c3** compressive strain 0.375
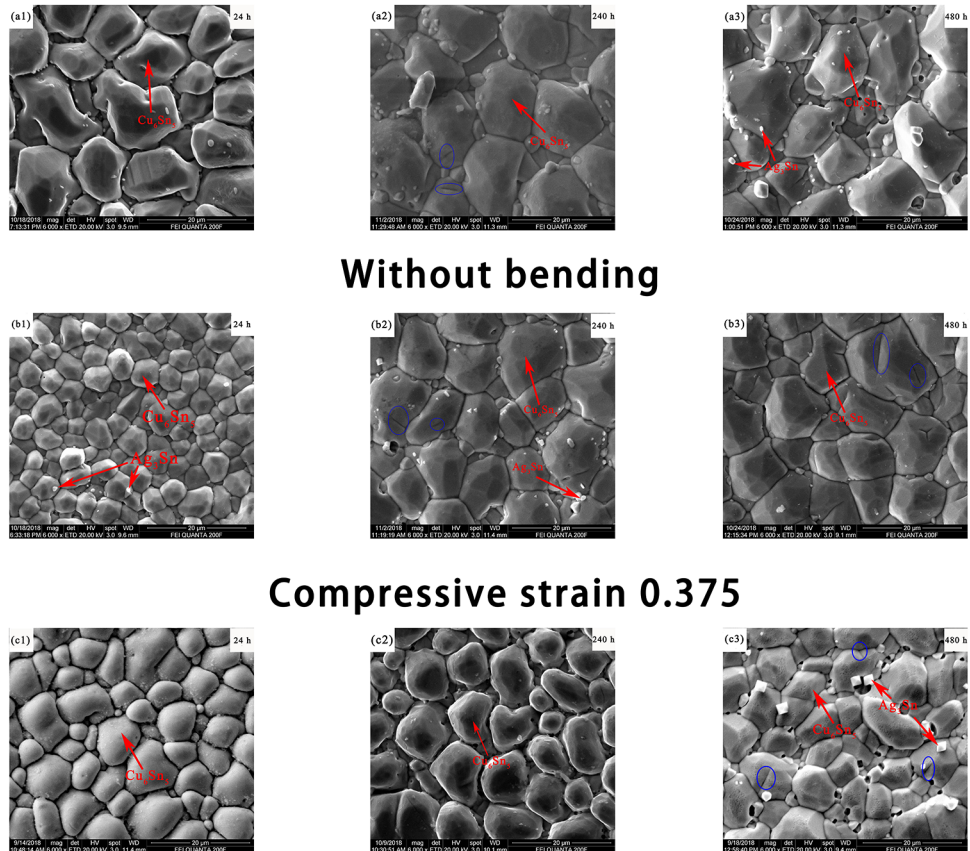
and discussions above, the following conclusions can be drawn:

(1) The thickness of both total IMCs and Cu_3Sn layer in SAC305/Cu solder joints under non-strained constantly increased with increased aging time. However, the thickness of Cu_6Sn_5 layer slightly decreased after aging for 120 h and increased as the aging time was prolonged to 480 h. It indicated that the growth rate of Cu_3Sn layer was faster than that of Cu_6Sn_5 layer within 120 h aging time. Besides, the round-shape Cu_6Sn_5 grains were observed in non-strained system after aging 24 h. As the aging time was prolonged, the morphology of Cu_6Sn_5 grains gradually changed from round-shape into polyhedron-shape and the mean size of Cu_6Sn_5 grain obviously increased.

(2) The applied tensile strain had an enhanced effect on the growth rate of the Cu_6Sn_5 and Cu_3Sn phases formed at the SAC305/Cu interface, regardless of strain value. The variation trend of the Cu_6Sn_5 layer thickness was the same as that of non-strained samples when the tensile strain value was 1.0 or 1.5%. In addition, the applied compressive strain inhibited the growth of Cu_6Sn_5 phase formed at the SAC305/Cu interface. The thickness of Cu_6Sn_5 IMC layer was not almost increased with increased aging time when the compressive strain value was 0.375%.

(3) The mean size of Cu_6Sn_5 grains under tensile or compressive strain was larger than that of non-strained sample after aging 24 h and slightly increased with prolonged aging time. The morphology of Cu_6Sn_5 grains was not change with increasing aging time and still was polyhedron-shape, regardless of strained type.

(4) The Kirkendall voids appeared within Cu_3Sn layer after aging for 120 h and the amount of voids gradually increased with prolonged aging time, regardless of whether strain was or not applied. The applied tensile or compressive strain had an enhanced effect on the formation of voids within Cu_3Sn layer and the enhanced effect of applied tensile strain was more remarkable than that of other systems.

References

1. C.Y. Lee, W.C. Moon, S.B. Jung, Surface finishes of rolled copper foil for flexible printed circuit board. Mater. Sci. Eng. A **483**(1), 723–726 (2008)
2. J.X. Wang, K.T. Chen, B.Z. Wen et al., Transesterification of soybean oil to biodiesel using cement as a solid base catalyst. J. Taiwan Inst. Chem. Eng. **43**(2), 215–219 (2012)
3. K.Z. Wang, C.M. Chen, Intermetallic compound formation and morphology evolution in the 95Pb5Sn flip-chip solder joint with Ti/Cu/Ni under bump metallization during reflow soldering. J. Electron. Mater. **34**(12), 1543–1549 (2005)
4. X. Hu, T. Xu, X. Jiang et al., Interfacial reaction and IMCs growth behavior of Sn3.0Ag0.5Cu/Ni solder bump during aging at various temperatures. J. Mater. Sci. **27**(5), 4245–4252 (2016)
5. X. Hu, T. Xu, L.M. Keer et al., Microstructure evolution and shear fracture behavior of aged Sn3.0Ag0.5Cu/Cu solder joints. Mater. Sci. Eng. A **673**, 167–177 (2016)
6. J.X. Wang, H. Nishikawa, Impact strength of Sn–3.0Ag–0.5Cu solder bumps during isothermal aging. Microelectron. Reliab. **54**(8), 1583–1591 (2014)
7. H. Nishikawa, N. Iwata, Formation and growth of intermetallic compound layers at the interface during laser soldering using Sn–Ag–Cu solder on a Cu Pad. J. Mater. Process. Technol. **215**(215), 6–11 (2015)
8. F. Wang et al., Recent progress on the development of Sn–Bi based low-temperature Pb-free solders. J. Mater. Sci. (2019). https://doi.org/10.1007/s10854-019-00701-w
9. Burke C, Punch J. A comparison of the creep behaviour of joint-scale SAC105 and SAC305 solder samples under shear conditions. IEEE Trans. Compon. Pack. Manuf. Technol. (2012)
10. F. Cheng, F. Gao, J. Zhang et al., Tensile properties and wettability of SAC0307 and SAC105 low Ag lead-free solder alloys. J. Mater. Sci. **46**(10), 3424–3429 (2011)
11. X. Hu, T. Xu, L.M. Keer et al., Microstructure evolution and shear fracture behavior of aged Sn3Ag05Cu/Cu solder joints. Mater. Sci. Eng. A **673**, 167–177 (2016)
12. M.N. Bashir, A.S.M.A. Haseeb, Improving mechanical and electrical properties of Cu/SAC305/Cu solder joints under electromigration by using Ni nanoparticles doped flux. J. Mater. Sci. **29**, 3182–3188 (2018)
13. C.P. Lin, C.M. Chen, C.H. Lin et al., Interfacial reactions of Sn/Ag/Cu tri-layer on a deformed polyimide substrate. J. Alloy. Compd. **502**(2), 17–19 (2010)
14. C.P. Lin, C.M. Chen, Y.W. Yen, Enhanced growth of the Cu_6Sn_5 phase in the Sn/Ag/Cu and Sn/Cu multilayers subjected to applied strain. J. Alloy. Compd. **591**, 297–303 (2014)
15. W.K. Liao, C.M. Chen, M.T. Lin et al., Enhanced growth of the Ni_3Sn_4 phase at the Sn/Ni interface subjected to strains. Scr. Mater. **65**(8), 691–694 (2011)
16. Y.J. Chen, C.M. Chen, Mitigative tin whisker growth under mechanically applied tensile stress. J. Electron. Mater. **38**(3), 415–419 (2009)
17. X. Zhang, X. Hu, X. Jiang et al., Effect of Ni addition to the Cu substrate on the interfacial reaction and IMC growth with Sn3.0Ag0.5Cu solder. Appl. Phys. A **124**(4), 315 (2018)
18. H. Li, R. An, C. Wang et al., In situ, quantitative study of microstructural evolution at the interface of Sn3.0Ag0.5Cu/Cu solder joint during solid state aging. J. Alloy. Compd. **634**, 94–98 (2015)
19. K.N. Tu, *Solder Joint Technology* (Springer, New York, 2007), p. 117
20. W.Q. Peng, E. Monlevade, M.E. Marques, Effect of thermal aging on the interfacial structure of SnAgCu solder joints on Cu. Microelectron. Reliab. **47**, 2161–2168 (2007)

21. L. Yin, P. Borgesen, On the root cause of Kirkendall voiding in Cu_3Sn. J. Mater. Res. **26**(03), 455–466 (2011)

22. C. Yu, Y. Yang, H. Lu, J.M. Chen, Effects of current stressing on formation and evolution of Kirkendall voids at Sn–3.5Ag/Cu interface. J. Electron. Mater. **39**, 1309–1314 (2010)

23. F.Y. Ouyang, C.L. Kao, In situ observation of thermomigration of Sn atoms to the hot end of 96.5Sn–3Ag–0.5Cu flip chip solder joints. J. Appl. Phys. **110**, 123525 (2011)

24. Y.W. Wang, Y.W. Lin, C.R. Kao, Inhibiting the formation of microvoids in Cu_3Sn by additions of Cu to solders. J. Alloy. Compd. **493**(1–2), 233–239 (2010)

25. J.Y. Song, J. Yu, T.Y. Lee, Effects of reactive diffusion on stress evolution in Cu–Sn films. Scr. Mater. **51**(2), 167–170 (2004)

26. R. Olender, A. Nitzan, Lattice theory of solvation and dissociation in macromolecular fluids II. Quasichemical approximation. J. Chem. Phys. **101**(3), 2338–2349 (1994)

27. C. Herring, Effect of change of scale on sintering phenomena. J. Appl. Phys. **21**(4), 301–303 (1950)

28. J. Shen, M. Zhao, H.E. Peipei et al., Growth behaviors of intermetallic compounds at Sn–3Ag–0.5Cu/Cu interface during isothermal and non-isothermal aging. J. Alloy. Compd. **574**(10), 451–458 (2013)

29. N. Bao, X. Hu, Y. Li et al., Effects of thermal aging on growth behavior of interfacial intermetallic compound of dip soldered Sn/Cu joints. J. Mater. Sci. **29**(10), 8863–8875 (2018)

30. Y. Lai, X. Hu, Y. Li et al., Interfacial microstructure evolution and shear strength of Sn0.7Cu–xNi/Cu solder joints. J. Mater. Sci.-Mater. Electron. **29**, 1–11 (2018)

31. X. Hu, T. Xu, X. Jiang et al., Effects of post-reflow cooling rate and thermal aging on growth behavior of interfacial intermetallic compound between SAC305 solder and Cu substrate. Appl. Phys. A **122**(4), 278 (2016)

32. H.K. Kim, K.N. Tu, Kinetic analysis of the soldering reaction between eutectic SnPb alloy and Cu accompanied by ripening. Phys. Rev. B **53**(23), 16027–16034 (1996)